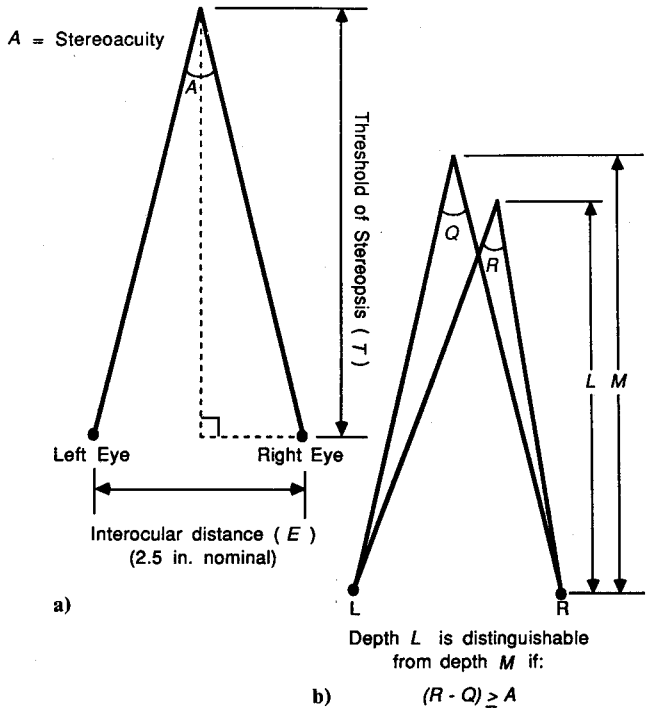

Fig. 1 Threshold of stereopsis and distinguishable depth.

and this fact bodes well for the widespread compatibility of stereopsis with flight simulators.

Future Research and Applications

The true value of stereopsis to flight simulation will require much further research. A state-of-the-art stereoscopic flight simulator is currently being built for the Army Research Institute. This system, called the Simulator Complexity Test Bed, features a helmet mounted display system with high-resolution area-of-interest insets. The CIG is stereo capable and software reconfigurable, meaning that the system can be configured to produce stereo views, or the same hardware can be configured to trade stereopsis for greater resolution and scene density or additional monoscopic channels. This will allow the evaluation of stereopsis without having to commit to running in stereo all of the time.

The future for stereoscopic flight simulators appears promising. Clearly, the tasks most likely to benefit from stereopsis are those in which objects are viewed at relatively close distances and/or where there is a scarcity of other depth cues. Such tasks as aerial refueling and formation flight require the pilot to acquire and maintain a precise position in close proximity to another aircraft without the benefit of the constant motion parallax present in other maneuvers. Low-speed nap-of-earth flight and landings require accurate distance perception to close range objects. Space operations, such as docking and manipulator arm operation, exemplify an application where all available cues are needed to successfully perform these slow, precise, and short range maneuvers with accuracy of fractions of an inch.

Conclusion

Advances in CIG and display technology now make it feasible to create stereoscopic out-the-window imagery for flight simulation. The results of testing to date indicate that, in simulators, stereopsis is a valid cue at distances of up to 300 ft and that stereopsis will enhance pilot performance in many training tasks. The true value of stereopsis to flight simulation will require studies using pilots in state-of-the-art stereoscopic simulators. Such systems are now being developed.

References

[1]Tidwell, R. P., "Stereopsis as a Visual Cue In Flight Simulation," *AIAA Flight Simulation Technologies Conference Technical Papers,* Aug. 1989, pp. 188–194.

[2]Yeh, Y., and Silverstein, L. D., "Depth Discrimination in Stereoscopic Displays," *Society for Information Display Digest of Technical Papers,* 1989, pp 372–375.

[3]Kruk, R. V., and Runnings, D. W., "Low Level Flight Performance and Air Combat Maneuvering Performance in a Simulator With a Fiber Optic Helmet Mounted Display System," AIAA Paper 89-3287, Aug. 1989.

[4]Busquets, A. M., Parrish, R. V., and Williams, S. P. "Depth-Viewing-Volume Increase by Collimation of Stereo 3-D Displays," *IEEE Southeastern 1990 Proceedings,* IEEE, New York, April 1990, pp. 589–593.

Comparison of One- and Two-Interface Methods for Tunnel Wall Interference Calculation

C. F. Lo* and N. Ulbrich†
The University of Tennessee Space Institute, Tullahoma, Tennessee 37388

Introduction

THE procedures of recently developed adaptive wall wind tunnels require a variety of flow variables to be measured near or on tunnel wall boundaries. These variables can be utilized to determine wall interference. Several wall interference calculation methods are available based on different kinds of boundary measurements. The NASA Ames Research Center 2-ft tunnel[1] has the capability to obtain these boundary measurements. Specifically, the pressure coefficient interference $c_{pi}(x,0)$ at the centerline of the tunnel can be determined based on the measurement of axial and vertical velocity components $u_t(x, \pm y_1)$ and $v_t(x, \pm y_1)$ on one interface named as method 1, or based on the measurement of vertical velocity components $v_t(x, \pm y_1)$ and $v_t(x, \pm y_2)$ alone on two interfaces named as method 2. The coordinates y_1 and y_2 describe the location of interfaces in the tunnel (see Fig. 1).

For small disturbances in a subsonic flowfield, $c_{pi}(x,0)$ is related to the axial interference velocity component $u_i(x,0)$ as follows

$$c_{pi}(x,0) = -2 \cdot u_i(x,0) \tag{1}$$

The interference velocity component $u_i(x,0)$ according to method 1 is given by Lo[2] and Dahm[3] in the following form

$$u_i(x,0) = \frac{\beta y_1}{2\pi} \int_{-\infty}^{\infty} \frac{u_t(\xi,y_1) + u_t(\xi,-y_1)}{(\xi - x)^2 + (\beta y_1)^2}\, d\xi$$

$$+ \frac{1}{2\pi\beta} \int_{-\infty}^{\infty} \frac{v_t(\xi,y_1) - v_t(\xi,-y_1)}{(\xi - x)^2 + (\beta y_1)^2} \cdot (\xi - x)\, d\xi \tag{2}$$

Received April 28, 1990; revision received May 19, 1990.

*Professor of Aerospace Engineering. Member AIAA.
†Graduate Research Assistant.

where $\beta = \sqrt{1 - M_\infty^2}$ and M_∞ is the free stream Mach number.

The corresponding equation for method 2 is given by Lo[4]

$$u_i(x,0) = \frac{-2}{\pi\beta}\left[\int_{-\infty}^{\infty} v_s(\xi,y_2)\cdot S_1\, d\xi - \int_{-\infty}^{\infty} v_s(\xi,y_1)\cdot S_2\, d\xi\right] \tag{3a}$$

where

$$v_s(\xi,y_1) = [v_t(\xi,y_1) - v_t(\xi,-y_1)]/2 \tag{3b}$$

$$v_s(\xi,y_2) = [v_t(\xi,y_2) - v_t(\xi,-y_2)]/2 \tag{3c}$$

$$S_1 = \sum_{k=1}^{\infty} \frac{x-\xi}{(x-\xi)^2 + [\beta y_1 + (2k-1)\beta(y_2-y_1)]^2} \tag{3d}$$

$$S_2 = \sum_{k=1}^{\infty} \frac{x-\xi}{(x-\xi)^2 + [\beta y_2 + (2k-1)\beta(y_2-y_1)]^2} \tag{3e}$$

Equations (2) and (3a) require a numerical integration, which can be computed more efficiently if the technique of integration by matrix multiplication is applied. This method works as follows:

The improper integrals used in Eqs. (2) and (3a) have the general form at the discrete x location x_i

$$I_i = \int_{-\infty}^{\infty} g(\xi,x_i)\cdot f(\xi)\, d\xi \tag{4}$$

where $f(\xi)$ is only a function of measurements at the interface and $g(\xi,x_i)$ just depends on geometrical parameters. Applying Simpson's rule, we get the following discrete equation, if we subdivide the interval $[-a,a]$ into $2m$ subintervals

$$I_i \approx \int_{-a}^{a} g(\xi,x_i)\cdot f(\xi)\, d\xi \approx \frac{a}{3m}\cdot[g(\xi_0,x_i)\cdot f(\xi_0) + 4\cdot g(\xi_1,x_i)\cdot f(\xi_1) + 2\cdot g(\xi_2,x_i)\cdot f(\xi_2) + \ldots + g(\xi_{2m},x_i)\cdot f(\xi_{2m})] \tag{5}$$

The integration limits $\pm a$ approach $\pm\infty$ for Eq. (4).

The improper integral can be evaluated at x_i for l discrete x locations. Therefore Eq. (5) can be expressed as a matrix multiplication given as

$$\boldsymbol{I} \approx G\cdot\boldsymbol{F} \tag{6a}$$

where

$$\boldsymbol{I}^T = [I_1, I_2, \ldots, I_l] \tag{6b}$$

$$G = \begin{pmatrix} (a/3m)g(\xi_0,x_1) & (4a/3m)g(\xi_1,x_1) & \ldots & (a/3m)(\xi_{2m},x_1) \\ (a/3m)g(\xi_0,x_2) & (4a/3m)g(\xi_1,x_2) & \ldots & (a/3m)(\xi_{2m},x_2) \\ \cdot & \cdot & \cdot & \cdot \\ \cdot & \cdot & \cdot & \cdot \\ \cdot & \cdot & \cdot & \cdot \\ (a/3m)g(\xi_0,x_l) & (4a/3m)g(\xi_1,x_l) & \ldots & (a/3m)(\xi_{2m},x_l) \end{pmatrix} \tag{6c}$$

$$\boldsymbol{F}^T = [f(\xi_0), f(\xi_1), f(\xi_2), \ldots, f(\xi_{2m})] \tag{6d}$$

Elements of vector $\boldsymbol{I}$ are approximated values of improper integrals, G is a $l \times (2m+1)$ matrix, and $\boldsymbol{F}$ is a vector depending only on measurements.

The coefficients of the matrix G can be calculated in advance. This simplifies and accelerates calculation procedures in on-line operation because the numerical integration has been reduced to a simple matrix multiplication. The reduction in CPU time is significant if the input of precalculated matrix coefficients is done in unformatted form. In this case, execution time is saved by eliminating the data translation process. One- and two-interface methods need approximately the same CPU time on a computer if Eqs. (3d) and (3e) are evaluated using Euler-MacLaurin's summation formula.[5]

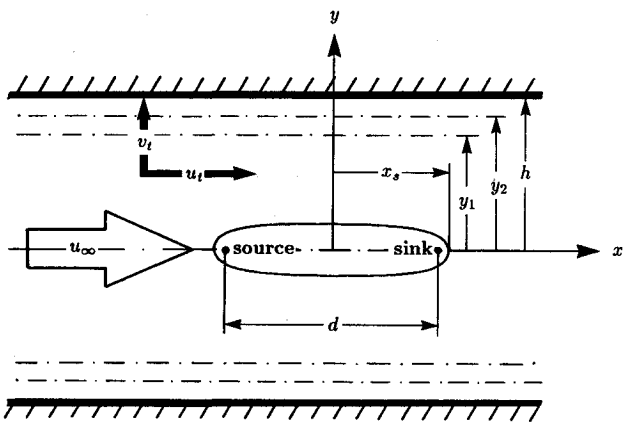

Fig. 1 Source/sink model in a closed wind tunnel.

Source/Sink Model

A closed wind tunnel with a source/sink model is shown in Fig. 1. As a numerical example, geometric parameters have been selected: tunnel half height $h = 1.0$, source/sink distance $d = 1.0$, stagnation point location $x_s = 0.52$, y coordinate first interface $y_1 = 0.65$, y coordinate second interface $y_2 = 0.80$. Based on the method of images, a theoretical value of $c_{pi}(x,0)$ and the axial and vertical velocity components $u_t(x,y)$ and $v_t(x,y)$ at any location (x,y) in an incompressible tunnel flowfield can be expressed in infinite series form and computed numerically.

The numerical values of u_t and v_t have been considered as ideal undisturbed measurements. Using these simulated measurements and Eqs. (1-3), the pressure coefficient interference $c_{pi}(x,0)$ can be calculated for the one- and two-interface methods and compared to the value obtained by applying the method of images. The values of $c_{pi}(x,0)$ show excellent agreement of calculated data based on Eqs. (1-3), and those data derived from the method of images for both methods. The results of the one-interface method are given in Fig. 2.

Comparison of the Sensitivity to Disturbed Measurements

The comparison of the sensitivity of both methods requires the generation of randomly disturbed measurements at interfaces. By assuming an amplitude δ and using different sets of random numbers $r(x)$ [where $0.0 \le r(x) \le 1.0$], a disturbance function $f_d(x)$ can be defined

$$f_d(x) = \delta \cdot [2 \cdot r(x) - 1] \tag{7}$$

Different sets of random numbers $r(x)$ will generate different sets of disturbance functions. These will be added to undisturbed ideal measurements that have been calculated based on the source/sink model as shown in Fig. 3. For the numerical comparison of the two methods, an amplitude of $\delta = 0.002$ has been selected and values of $c_{pi}(x,0)$ have been calculated for various sets of random numbers. Calculated results are presented in Figs. 4 and 5 using method 1 and method 2, respectively. The solid line represents the ideal analytical value of $c_{pi}(x,0)$ based on the source/sink model. The dashed lines represent the calculated values of $c_{pi}(x,0)$ based on disturbed measurements. Comparing results of both methods, it is obvious that method 1 is less sensitive to random disturbances and hence it becomes more attractive for practical applications. A similar observation is given by Schairer and Lee.[1] The unfavorable behavior of method 2 is probably caused by the measurement of vertical velocity components at interfaces. For the same amplitude δ, the relative error $\delta/|v_t|$ is significantly larger than the relative error $\delta/|u_t|$.

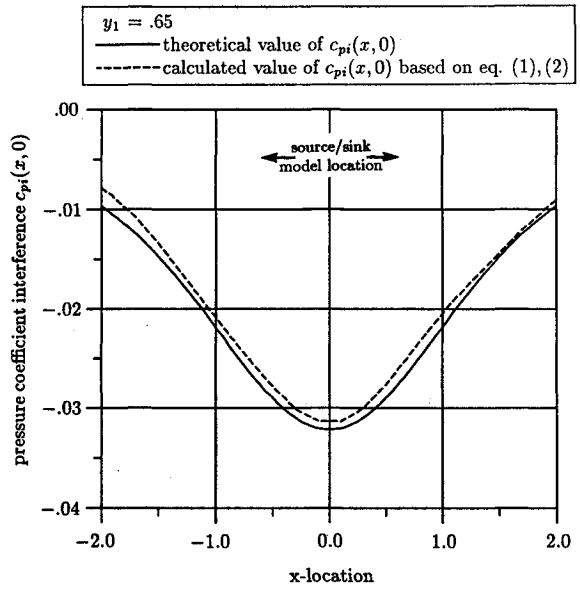

Fig. 2 Pressure coefficient interference distribution based on a source/sink model flowfield compared to values obtained from the one-interface method.

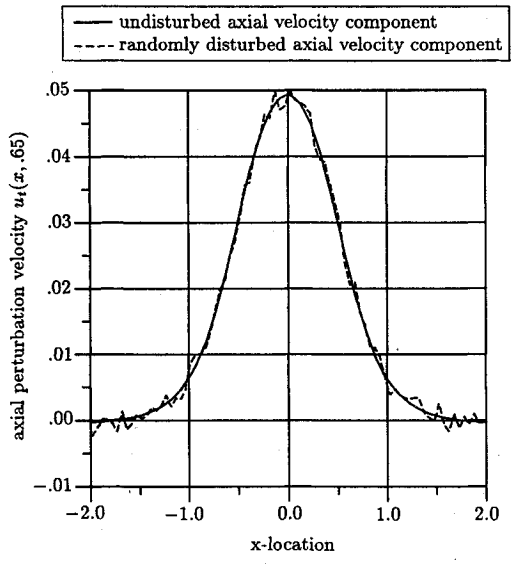

Fig. 3 Undisturbed and randomly disturbed (disturbance amplitude $\delta = 0.002$) axial velocity distribution at the interface location $y_1 = 0.65$.

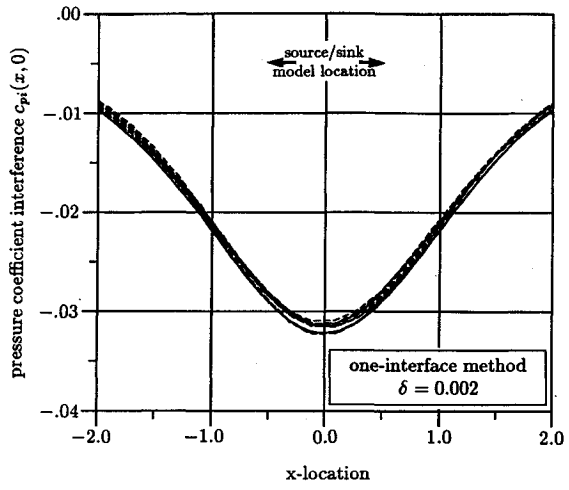

Fig. 4 Pressure coefficient interference calculated based on the one-interface method with disturbance amplitude $\delta = 0.002$.

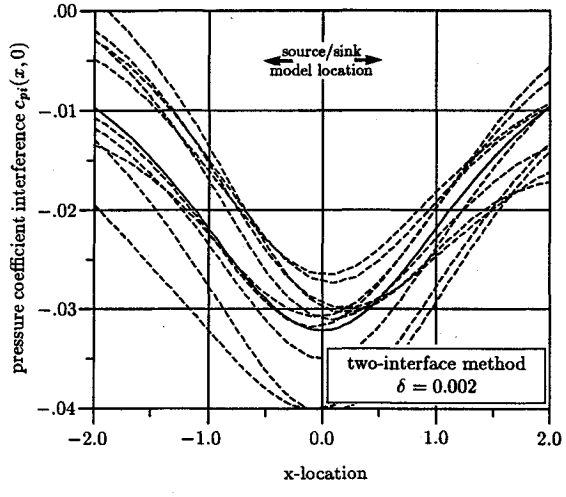

Fig. 5 Pressure coefficient interference calculated based on the two-interface method with disturbance amplitude $\delta = 0.002$.

Concluding Remarks

Tunnel wall interference in two-dimensional subsonic flow can be calculated analytically based on the one- or two-interface method. Applying the technique of numerical integration by matrix multiplication to both methods, it was possible to reduce the CPU time in on-line operation significantly. The sensitivity of both methods to random disturbances of velocity measurements has been studied. The comparison of results has shown that the one-interface method is less sensitive to the error of measurements and hence is the preferable one for practical applications. Another way to investigate the sensitivity of one- and two-interface methods is the calculation of the uncertainty propagation,[6] which may be used for the study in the future.

Acknowledgment

This research was partially supported by NASA Grant NAG 2-551 and University of Tennessee-Calspan Center for Aerospace Research. Frank W. Steinle Jr. was the grant technical monitor.

References

[1]Schairer, E. T., and Lee, G., "Two-Dimensional Adaptive-Wall Tests in the AMES Two-by-Two-Foot Transonic Wind Tunnel," to appear in *Journal of Aircraft*.

[2]Lo, C. F., "Tunnel Interference Assessment by Boundary Measurements," *AIAA Journal*, Vol. 16, No. 4, 1978, pp. 411–413.

[3]Dahm, W., "A General Solution for Wind Tunnel Boundary-Induced Interference in Two-Dimensional Subsonic Flow," The University of Tennessee, Knoxville, TN, March 1981, p. 35.

[4]Lo, C. F., "Tunnel Interference Assessment from Measurements on Two Interfaces," to appear in *AIAA Journal*.

[5]Dahlquist, G., and Björck, Å., *Numerical Methods,* translated by N. Anderson, Prentice-Hall, Englewood Cliffs, NJ, 1974, p. 73.

[6]Abernethy, R. B., and Thompson, J. W., "Uncertainty in Gas Turbine Measurements," AEDC TR-73-5, 1973.